Three-dimensional simulations of the accretion process in Kerr space-time with arbitrary value of the spin parameter

Cosimo Bambi[*] and Naoki Yoshida[†]

Institute for the Physics and Mathematics of the Universe, The University of Tokyo, Kashiwa, Chiba 277-8583, Japan
(Received 26 June 2010; published 2 September 2010)

We present the results of three-dimensional general relativistic hydrodynamic simulations of adiabatic and spherically symmetric accretion in Kerr space-time. We consider compact objects with spin parameter $|a_*| \leq 1$ (black holes) and with $|a_*| > 1$ (superspinars). Our full three-dimensional simulations confirm the formation of equatorial outflows for high values of $|a_*|$, as found in our previous work in 2.5 dimensions. We show that the critical value of $|a_*|$ determining the onset of powerful outflows depends mainly on the radius of the compact object. The phenomenon of equatorial outflows can hardly occur around a black hole and may thus be used to test the bound $|a_*| \leq 1$ for astrophysical black hole candidates.

I. INTRODUCTION

It is widely believed that the final product of gravitational collapse is a Kerr black hole: an object with an event horizon that is completely characterized by two parameters, the mass M and the spin J. The condition for the existence of the event horizon is $|a_*| \leq 1$, where $a_* = J/M^2$ is the dimensionless spin parameter. The black hole paradigm relies on three ingredients. The first is that, in general relativity, under apparently reasonable assumptions, the collapsing matter forms space-time singularities [1]. The second one is the cosmic censorship conjecture [2], according to which all the space-time singularities must be hidden behind an event horizon. The last ingredient is the fact that in 4-dimensional general relativity the Kerr space-time is the only asymptotically-flat and stationary solution with a regular event horizon [3,4].

The cosmic censorship conjecture is a simple requirement to get rid of pathological space-times with unphysical properties. However, it seems to be motivated by our poor knowledge of the theory at high energy rather than by true physical reasons. Space-times with naked singularities may indeed arise from the break down of our theories at high energy. Instead of naked singularity, we might thus talk about effective naked singularity [5,6]: a space-time region outside an event horizon in which classical general relativity cannot be used and the future predictability is lost without the theory of quantum gravity. It is also remarkable that we know several counterexamples violating the cosmic censorship conjecture (see e.g. Refs. [7–12]).

In absence of an event horizon, there is no uniqueness theorem and, in general, the final product of the collapse is not as simple as a Kerr black hole. Nevertheless, as a first approximation, the space-time around the compact object can still be described by M and J if higher order multipole moments are subdominant. *The simplest test to rule out the Kerr black hole as the final product of the gravitational collapse is thus to find a massive and compact object with $|a_*| > 1$ (superspinar).* The idea that the end state of the collapse could violate the bound $|a_*| \leq 1$ was suggested in [13]. For the possibility of over-spinning an existent black hole, see e.g. Ref. [14]. The properties of the electromagnetic radiation emitted around Kerr superspinars were studied in [15–17] and compared with the case of Kerr black hole, in order to examine how to test the bound $|a_*| \leq 1$ with future experiments.

The accretion process onto Kerr superspinars in 2.5 dimensions (2 spatial dimensions, vectors with 3 spatial components) has been studied in [18–20]. Close to the object, the gravitational force can be repulsive. In Ref. [20], we discussed the Bondi accretion and found the formation of equatorial outflows. These outflows are very different from the one expected in the accretion process onto black holes: they are produced by the repulsive gravitational force at short distances, rather than by magnetic fields, and the gas is ejected on and around the equatorial plane, while in the black hole case the outflows are expected parallel to the spin. Current observations cannot directly probe if outflows and jets observed in black hole candidates are perpendicular or parallel to the spin of the massive objects, most of jets from radio galaxies appear to be of dipolar shape, being very different from planar outflows.

In this paper, we extend the work of Ref. [20]. We study the accretion process in 3 spatial dimensions. The main aim is to understand the structure of these outflows on the equatorial plane, which cannot be investigated in 2.5 dimensions. Indeed, one may naively expect roughly the following three basic configurations: (i) a perfect axial symmetry, in which the gas is ejected isotropically in all the directions, (ii) the formation of a certain number of collimated and stable outflows on the equatorial plane, or (iii) a strongly chaotic phenomenon, in which the accreting

---
[*]cosimo.bambi@ipmu.jp
[†]naoki.yoshida@ipmu.jp

material is ejected randomly along several directions and there is no formation of stable outflows. Our simulations suggest the third case.

The paper is organized as follows. In Sec. II, we discuss the model for superspinars. In Sec. III, we present the results of our 3-dimensional general relativistic hydrodynamic (3D GRHD) simulations. In particular, we show the cases of Schwarzschild black hole ($a_* = 0$), extreme Kerr black hole ($a_* = 1$), and Kerr superspinar with $a_* = 2$ and 3. In Sec. IV, we discuss the results. In Sec. V, there are summary and conclusions. Throughout the paper we use Boyer-Lindquist coordinates to describe the Kerr background and natural units $G_N = c = k_B = 1$.

II. SUPER-SPINAR MODEL

The Kerr space-time with $|a_*| > 1$ has a naked singularity at $r = 0$. For $r > 0$, the space-time is everywhere regular. The singularity at $r = 0$ is pointlike, but has the topology of a ring: it can connect our Universe, where $r > 0$, with another Universe, at $r < 0$. The problem is that an observer at $r > 0$ can go to the other Universe and, in absence of an event horizon, come back to our Universe at an earlier time; that is, the naked singularity can be used as a time machine [21]. However, one may expect that general relativity breaks down before reaching the singularity and that eventually causality cannot be violated. In absence of the complete theory of quantum gravity, we have to take a phenomenological approach to study the astrophysical properties of superspinars. Here we consider Kerr superspinars and we assume they can be modeled as a massive object with a radius $r \approx 2.5M$, whose surface absorbs all the accreting matter hitting it (the possibility of a surface with different properties is briefly discussed in Sec. IV). Our model is motivated by the following simple considerations.

(1) Roughly speaking, pathological regions with closed timelike curves can be removed by exciting the space-time. This occurs, for example, if the space-time goes to a new phase and a domain wall is formed [22–25]. Across the domain wall, the metric is nondifferentiable and the expected region with closed timelike curves arises from the naive continuation of the metric ignoring the domain wall. The latter can be made of very exotic stuff, e.g. supertubes [22,24,25] or fundamental strings [23].

(2) A crucial point is the radius of the new object. Here we take $r \approx 2.5M$ in order to prevent the instability of the superspinar [26] and have all the thermodynamical variables under control. For smaller/larger radii, one can properly rescale (decrease/increase) the spin parameter to obtain a very similar accretion process. For astrophysical bodies, M is a length much larger than the Planck scale $L_{Pl} \sim 10^{-33}$ cm, where quantum gravity effects are often expected. However, the gravitational radius $r_g \sim M$, rather

than L_{Pl}, may be the critical quantity. This occurs, for example, in the fuzzball picture [27]: here black holes have no horizon and the central singularity is replaced by a long string spreading over the volume classically occupied by the black hole. Even if so far only a few very special black holes have been studied, if correct, the fuzzball picture should be applied (somehow) even to the final product of the collapse of a star. The latter may thus resemble more a star made of very exotic matter than a black hole. However, unlike recent proposals such as boson stars, general relativity may not hold inside the object.

(3) In this work, we use the Kerr metric, which is described only by two parameters, M and J. In absence of an event horizon, one should instead expect a more complex object. Even if that is true, M and J are more likely the dominant terms in the multipole moment expansion and determine the main features of the accretion process.

III. 3D SIMULATIONS

In this section, we present the results of our 3D simulations in Kerr space-time with arbitrary value of the spin parameter a_*; for previous works on the accretion process in full general relativity, see e.g. Refs. [28–31]. The code is a revised version of the one used in [18–20]. Now the (default) computational domain is $2.5M < r < 40M$, $0 < \theta < \pi$, and $0 < \phi < 2\pi$. Unlike in [18–20], the thermodynamical variables are everywhere under control and we do not need to impose a maximum temperature. The accretion process is adiabatic. We assume an ideal nonrelativistic gas with $\Gamma = 5/3$, which is injected into the computational domain from the outer boundary at a constant rate and isotropically. We also examine several cases with $\Gamma = 4/3$ for relativistic particles. The gravitational field of the accreting matter is neglected (test fluid approximation). The initial conditions are the same of Refs. [18–20]. In the next subsections, we present the results of the simulations for a few different values of the spin parameter. The simulations run from $t = 0$ to $t = 500M$ (for $a_* = 0$, 1, and 2) or $t = 300M$ (for $a_* = 3$). We did not find always a quasi-steady-state configuration within this period. However, it seems to be enough to catch the main features of the accretion process.

A. Schwarzschild black hole ($a_* = 0$)

This is the simplest case. The accretion process is almost perfectly spherically symmetric, see Fig. 1. At the inner boundary $r_{in} = 2.5M$ and at $t = 500M$, our code predicts a temperature $T \approx 125$ MeV and a velocity $v = \sqrt{\gamma_{ij} v^i v^j} \approx 0.8$, where γ_{ij} is the 3-metric.

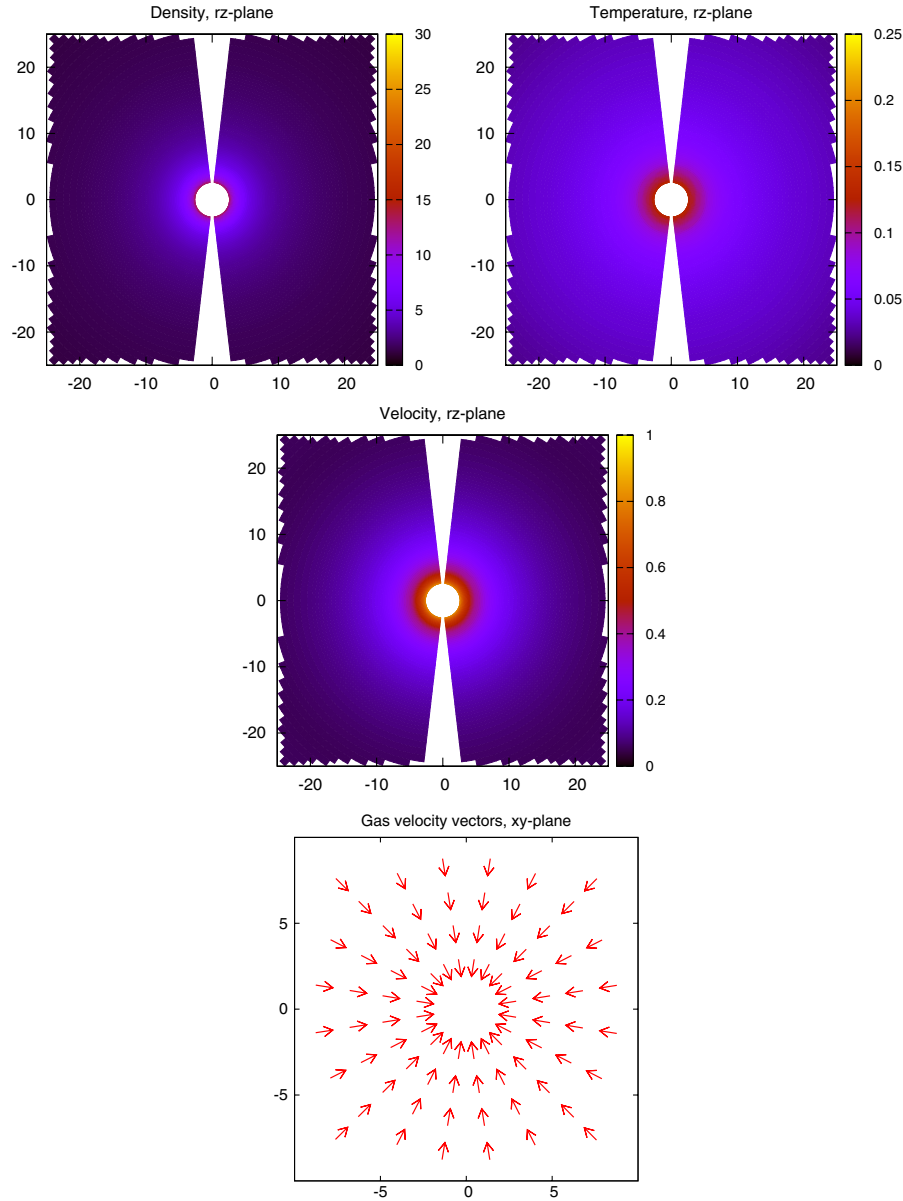For a Schwarzschild black hole, the general relativistic Bondi solutions are well known [32] (see also Appendix G

FIG. 1 (color online).   We plot the density ρ (in arbitrary units), the temperature T (in GeV), and the velocity $v = \sqrt{\gamma_{ij} v^i v^j}$ of the accreting gas around a Schwarzschild black hole ($a_* = 0$) at $t = 500M$. The bottom panel shows the direction of the gas velocity. The xy-plane is the equatorial plane, while the rz-plane is a plane containing the axis of symmetry z. The unit of length along the axes is M.

of Ref. [33]). The master equations are

$$4\pi r^2 \rho u = \text{const},\tag{1}$$

$$\left(1 - \frac{2M}{r} + u^2\right)h^2 = \text{const},\tag{2}$$

together with an equation of state. Here ρ is the rest-mass energy density, $h = 1 + \epsilon + p/\rho$ the specific enthalpy, ϵ the specific internal energy density, p the pressure, and $u = -u^r$ with u^r the radial component of the 4-velocity of the gas. We can thus compare the results of our numerical simulations with the Bondi solutions. Note, however, that

the two results do not have to match perfectly everywhere, because they are set up in a different way: in our simulations, we assume an initial gas distribution, we evolve the system, and we find a quasi–steady-state flow (for $a_* = 0$, this is achieved at $t \approx 300M$); in the Bondi case, one assumes from the beginning that the flow is in a quasi--steady-state configuration. The comparison is shown in Fig. 2. The initial configuration assumed in this work is a static cloud of gas around the massive object. We then inject gas from the outer boundary at a constant rate. Interestingly, the quasi-steady-state solution we found is close to the supersonic Bondi solution near the black hole, and approaches the subsonic Bondi solution near the outer
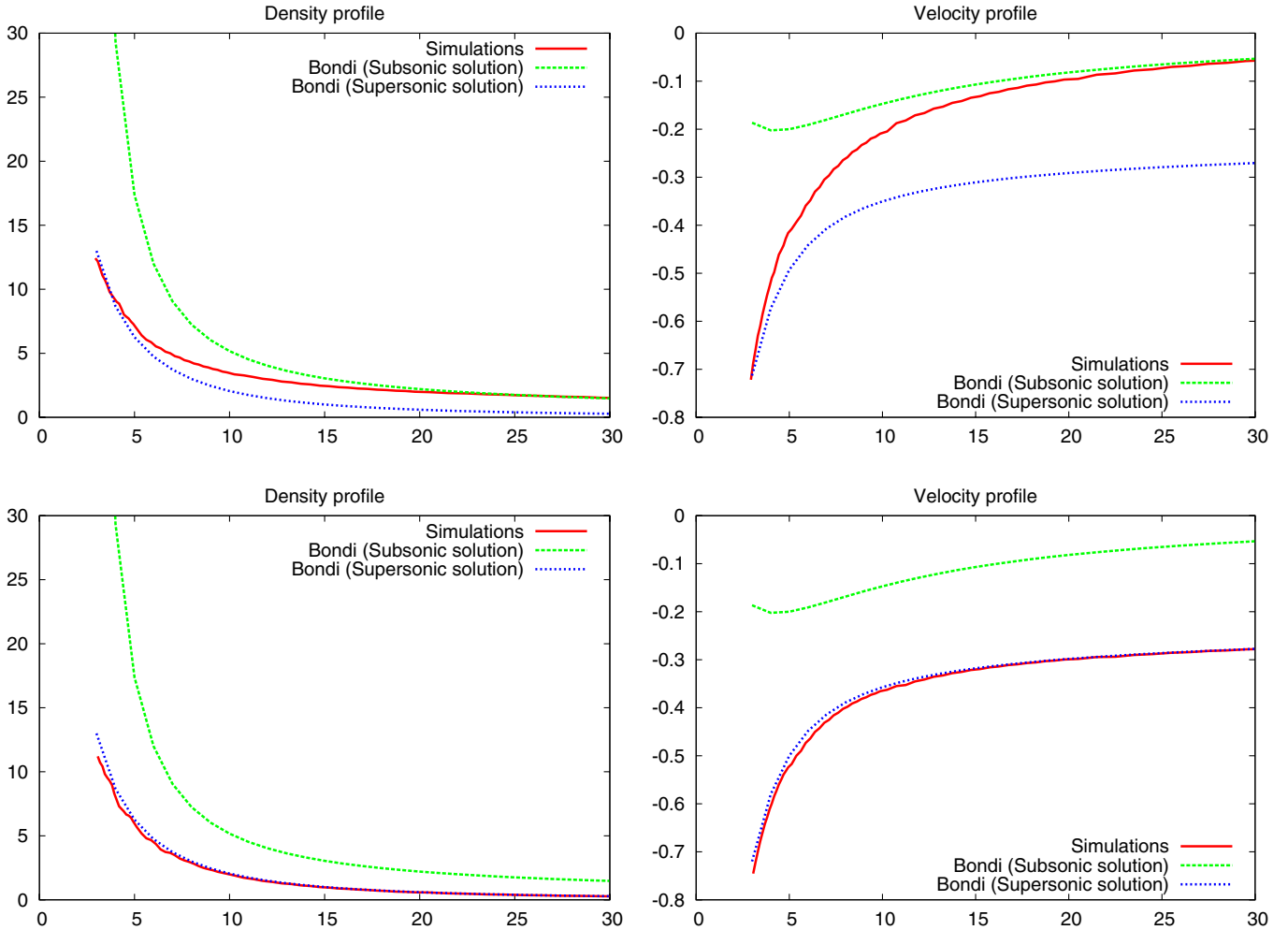
FIG. 2 (color online). Comparison of the density profile and of the radial velocity profile (as seen by a local observer) for $a_* = 0$, between our numerical simulations at $t = 500M$ and the semianalytical solutions of the relativistic Bondi equations. Assuming the initial gas distribution adopted in the simulations of this work, we find that the numerical solution is close to the supersonic solution at small radii and to the subsonic solution at larger radii (top panels). If we take the computational domain initially empty and we inject gas from the outer boundary, we can find a numerical solution close to the supersonic solution everywhere (bottom panels).

boundary (Fig. 2, top panels). A numerical solution quite similar to the Bondi ones can instead be reached by assuming that the computational domain is initially empty, and by injecting gas from the outer boundary at a proper density, pressure, and velocity (Fig. 2, bottom panels). The close agreement between the simulation results and the analytic solution is rather encouraging.

B. Extreme Kerr black hole ($a_* = 1$)

As we can see from Fig. 3, the accretion process onto an extreme Kerr black hole is still very similar to the Schwarzschild case. Now the density, the temperature, and the velocity of the gas are a little higher near the equatorial plane than near the axis of symmetry; however, the difference can be hardly appreciated. At r_{in}, the temperature is in the range 130–140 MeV and the velocity is $v \approx 0.7$. The latter is lower than the previous case, but we

have also to consider that now the horizon is at $r_H = M$, while, for $a_* = 0$, we had $r_H = 2M$. Let us notice that the computational domain does not include the ergoregion and that the velocity of the gas is essentially radial even near the inner boundary. The volume between r_{in} and the horizon r_H is, however, very small, and thus would not introduce any new interesting observational feature; indeed, most of the works in the literature use a pseudo–Newtonian potential, which neglects the spin of the massive object, and excludes the ergoregion from the computational domain. It is important to notice that in the case of black hole, the thermodynamical variables at any radial coordinate r are independent of the choice of r_{in}. To be more precise, that is generically true when the flow around the massive object is supersonic; that is, $r_{in} < r_s$, where r_s is the radius of the sonic point. Here, at $t = 500M$, we find $r_s \approx 6M$.
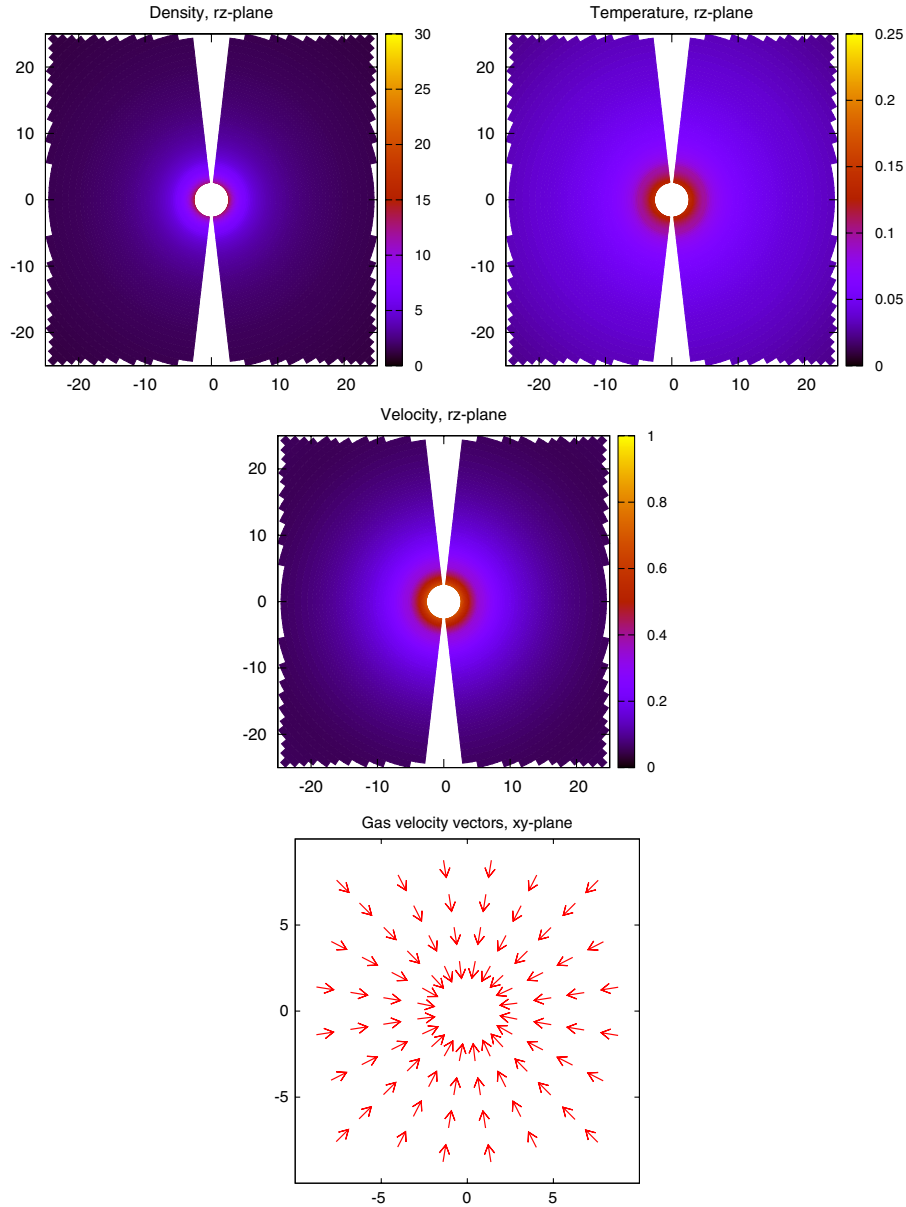
FIG. 3 (color online).   As in Fig. 1, but for an extreme Kerr black hole ($a_* = 1$).

C. Kerr superspinar with $a_* = 2$

The accretion process for $a_* = 2$ is shown in Fig. 4. For $r_{in} = 2.5M$, we exclude from the computational domain the region with repulsive gravitational force.[1] Despite that, the force is weaker than around a black hole and the accretion process is inefficient. The result is that the velocity of the accreting gas is lower, while the density and the temperature are higher. At the inner boundary r_{in}, we find that the velocity v is about 0.3 and the temperature is in the range 160–200 MeV. Now small variations of r_{in} can change the accretion process, because the flow is subsonic and the thermodynamical variables at larger radii can depend on the ones at smaller radii. As shown in the bottom panel of Fig. 4, near the center the effect of the spin is relevant and the gas is forced to corotate with the superspinar. In particular, we observe stable inflows forming a spiral structure, see Fig. 5.

D. Kerr superspinar with $a_* = 3$

For $a_* = 3$, the accretion process is significantly different from the cases discussed in the previous subsections. The difference can be clearly seen in Fig. 6. The gas can reach the surface of the superspinar from the poles, while the region around the equatorial plane is characterized by

---

[1]As discussed in [18,19], the region around the superspinar with repulsive gravitational force is roughly given by the expression $r < M|a_*||\cos\theta|$.
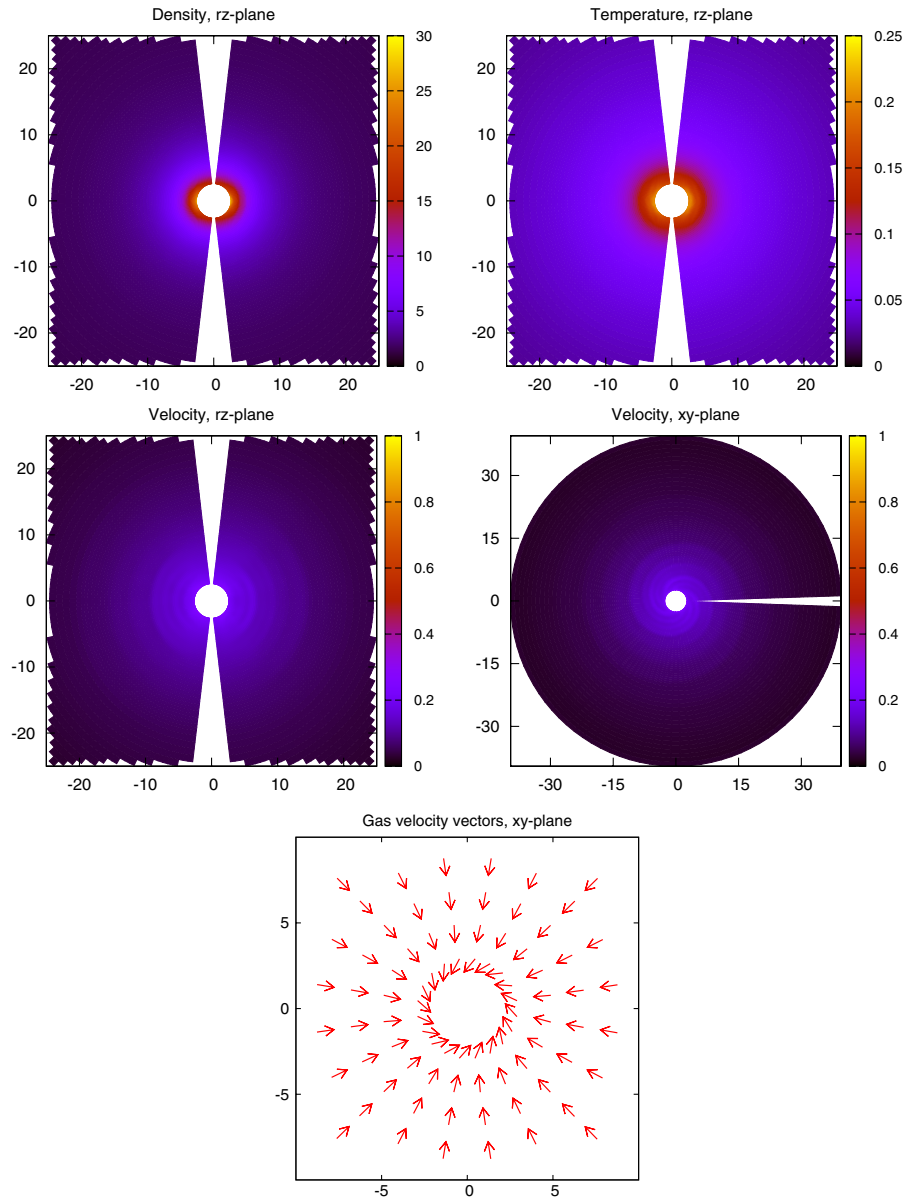
FIG. 4 (color online).   As in Fig. 1, in the case of a Kerr superspinar with $a_* = 2$.
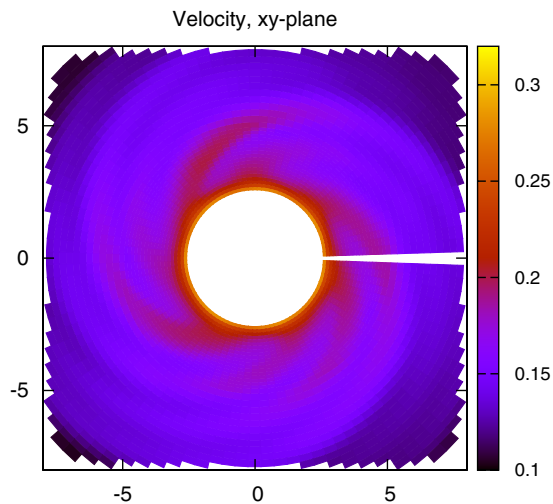

FIG. 5 (color online).   For $a_* = 2$, we find stable inflows forming a spiral structure. Such a feature is essentially absent when we plot the density or the temperature of the gas.
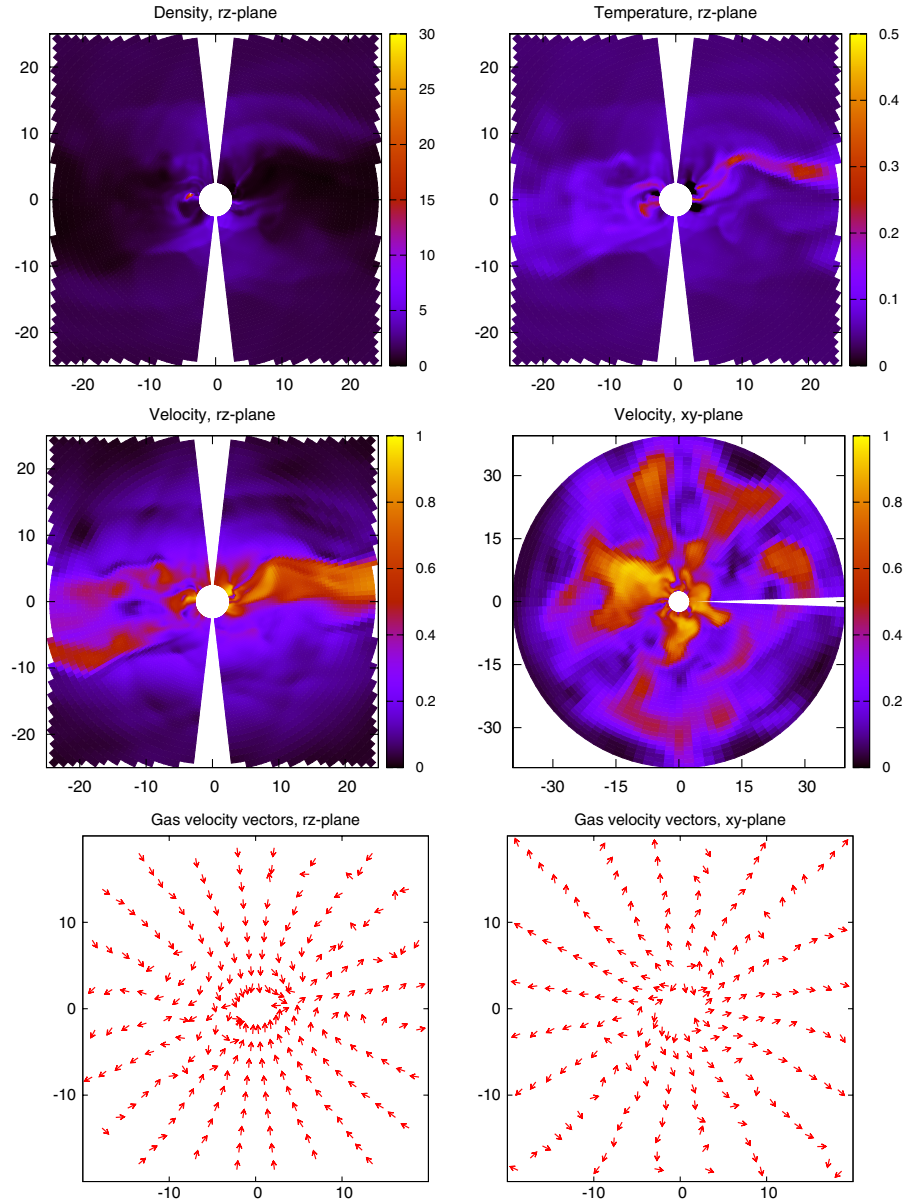
FIG. 6 (color online). As in Fig. 1, in the case of a Kerr superspinar with $a_* = 3$ and at $t = 300M$.

low-density, high-temperature outflows. This confirms the results found in [20] and shows the behavior of the gas along the third spatial coordinate. We do not find the formation of collimated and stable outflows, but a quite chaotic process of ejection of gas. The maximum temperature of the gas is in the range 400–700 MeV, but most of the gas is much cooler. The velocity of the gas in the outflows is found to be close to 1.

IV. DISCUSSION

On the basis of our simulations, we can see that the accretion process is more efficient onto objects with small spin parameter. As $|a_*|$ increases, it gets more and more difficult to make all the accreting gas be swallowed by the compact object. Eventually the repulsive gravitational force becomes strong enough to produce powerful equatorial outflows. In these 3D simulations we do not find a perfect axial symmetry, but find that the formation of outflows is a quite chaotic phenomenon. These are the main features of accretion in Kerr spacetime.

The transition between the three qualitatively different states (black holelike state, intermediate state, superspinarlike state) is rapid, but not instantaneous. To see this, in Fig. 7 we show the temperature and the velocity profile on the equatorial plane and along the axis of symmetry for $r_{in} = 2.5M$ and at $t = 500M$. The cases $a_* = 0$, 1, and 1.5 are quite similar. When $a_* = 2$, the attractive gravitational force around the massive object is not strong and the accretion process is less efficient: the velocity of the gas decreases significantly, while the temperature in-
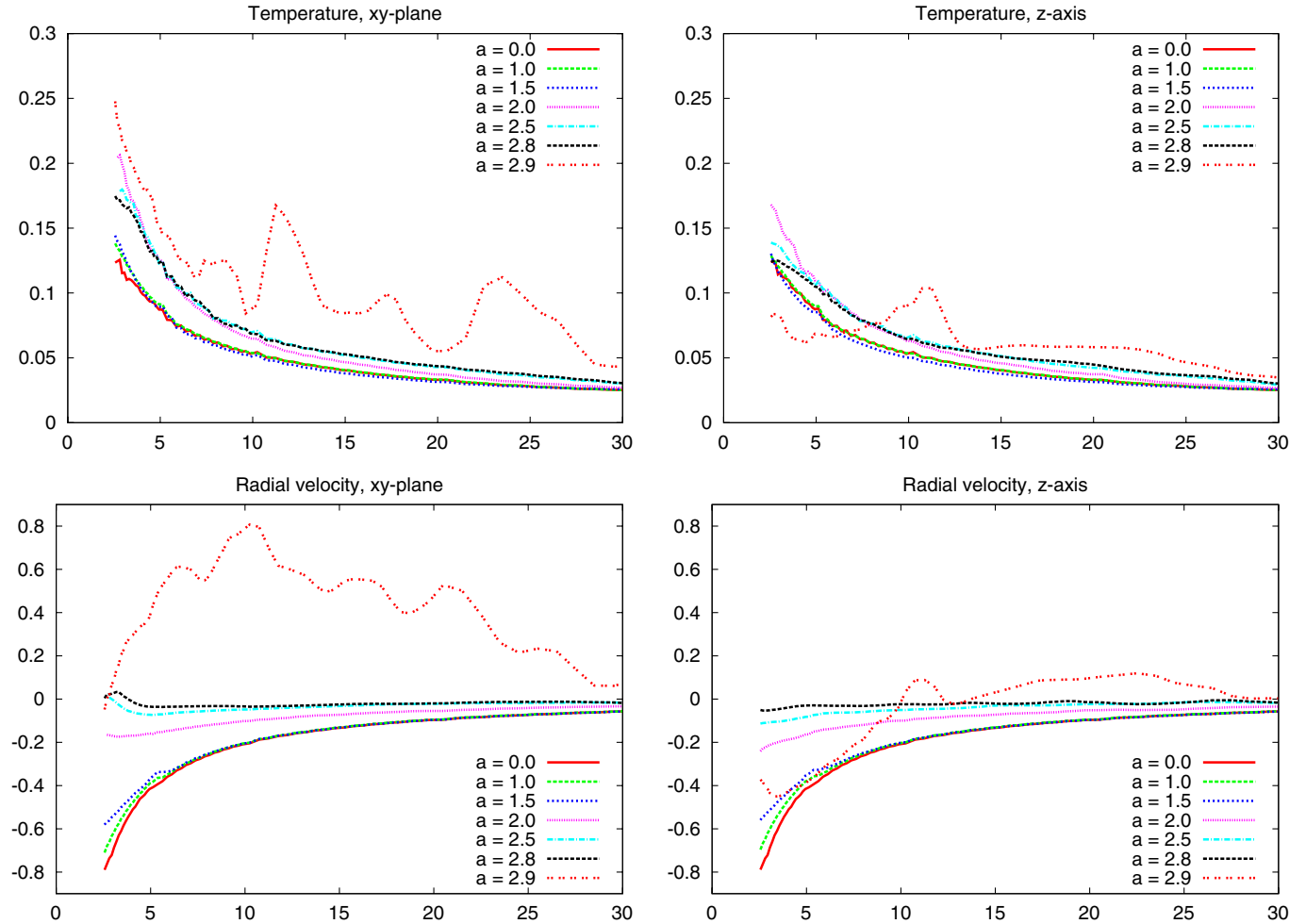
FIG. 7 (color online).   Temperature and radial velocity (as seen by a local observer) as a function of the radial coordinate on the equatorial plane (xy-plane) and along the z-axis of the accreting gas in Kerr space-time at $t = 500M$, for different values of a_*. $r_{in} = 2.5M$, temperature in GeV, radial coordinate in units $M = 1$. For $a_* = 0$, 1, and 1.5, we find a black hole-like accretion; for $a_* = 2$, an intermediate accretion; for $a_* = 2.9$, the accretion is of superspinar type. For $a_* = 2.5$ and 2.8, the accretion is essentially of the second kind, but there is some very weak ejection of matter near the equatorial plane.

creases. The flow around the massive object becomes subsonic. For $a_* \sim 2.5$, the region with repulsive gravitational force appears in the computational domain. We then see weak outflows on the equatorial plane. The outflow is so weak that it cannot go far from the massive object, but is instead pushed back by the accreting gas. As the spin parameter increases, the energy of the outflows increases as well. For $a_* = 2.9$, the outflows can reach the outer boundary of the computational domain at $r_{out} = 40M$. We have checked that, for a smaller/larger r_{in}, qualitatively the same behavior is found with a lower/higher value of the spin parameter. For example, setting $r_{in} = 3.0M$, weak equatorial outflows start forming for $a_* \sim 3.5$ and they becomes powerful when $a_* = 3.8$. The two key elements of the accretion process are thus the spin parameter and the radius of the massive object. The latter is replaced by the radius of the inner boundary in our simulations. A minor role is played by the initial and boundary conditions, like

the temperature and the velocity of the gas, i.e. by non-gravitational physics.

The mass of the accreting gas around the massive object, M_{gas}, or correspondingly the mean density ρ_{gas}, could be used as order parameter of the system. In the black hole state of accretion, these two quantities slightly increase as a_* increases. In the intermediate state, the mass and the density around the massive object reach a maximum, while, as soon as outflows can be produced, they drop to lower values. In Fig. 8, we show, as a function of the spin parameter a_*, the mean density of the accreting gas in the region $2.5M < r < 5.0M$ (left panel) and $2.5M < r < 10.0M$ (right panel) and at the time $t = 500M$. This fact can, however, unlikely be used in observations, because the mass and the density of the gas around the compact object are mainly determined by the accretion rate at larger distances. Here we simply note that, for the same initial and boundary conditions, the spin of the massive object
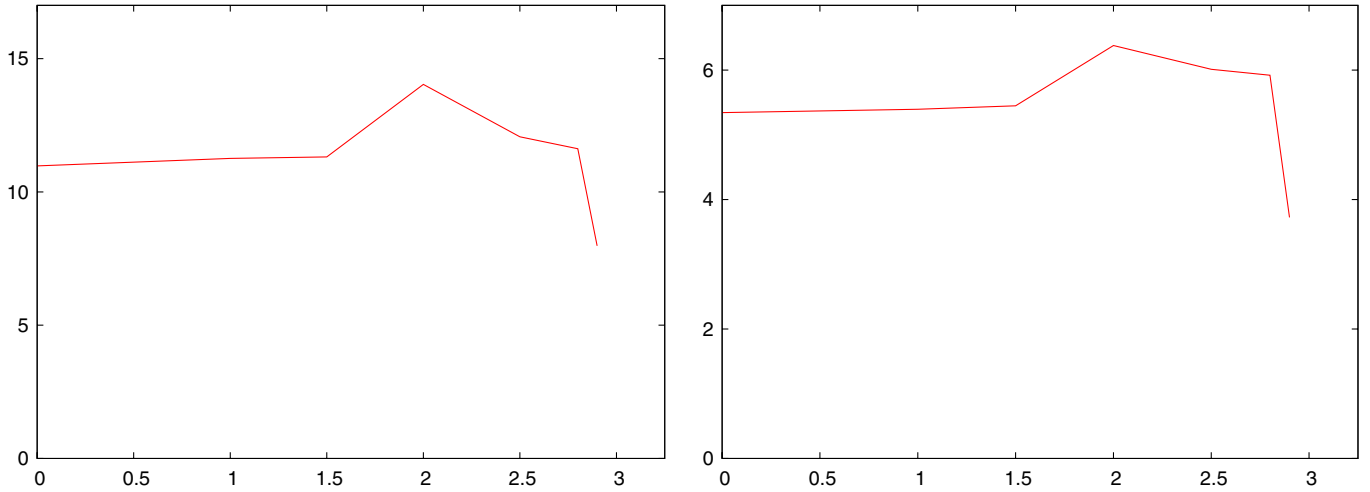
FIG. 8 (color online). Mean density of the accreting gas (in arbitrary units) around the massive object at $t = 500M$ as a function of the spin parameter a_*. Left panel: space region $r_{in} < r < 5M$. Right panel: space region $r_{in} < r < 10M$.

determines the amount of gas around the center as shown in Fig. 8.

In our superspinar model, the surface of the massive object absorbs all the accreting matter. Namely, we have assumed a transmission coefficient $T = 1$ and, consequently, a reflection coefficient $R = 1 - T = 0$. In this case, the surface of the superspinar would be similar to an event horizon, in the sense that it can swallow all the matter with no difficulties. The properties of the surface of the superspinar should depend on how the ordinary matter of the gas, made of protons and electrons, interacts with the exotic structure of the superspinar. The opposite case of a perfectly absorbing surface is a perfectly reflecting surface with $T = 0$ and $R = 1$ (rigid wall). To see the behavior of the accretion process with radically different properties of the surface of the superspinar, we run the code imposing reflective boundary conditions at r_{in}. For black holes and superspinars with low spin parameter, we found a quite obvious result: a dense cloud is formed around the massive object, which quickly explodes. For superspinars with moderate and high spin parameter, the system is much more stable, thanks to the nonspherical symmetry of the gravitational field. Now there is not the formation of the unstable cloud, since the gas around the massive object is efficiently expelled in the outflows: the gas reaches the surface of the superspinar from the poles, there is no accretion at all, because of the perfectly reflecting surface, and is ejected around the equatorial plane. We argue that the final result is the formation of a convective zone, where the gas continuously approaches and leaves the superspinar. In a more general case, one could expect that either T and R are nonzero, smaller than 1, and depend on the energy of the incident particle, i.e. $T = T(\omega)$ and $R = R(\omega)$. In any case, outflows on the equatorial plane for
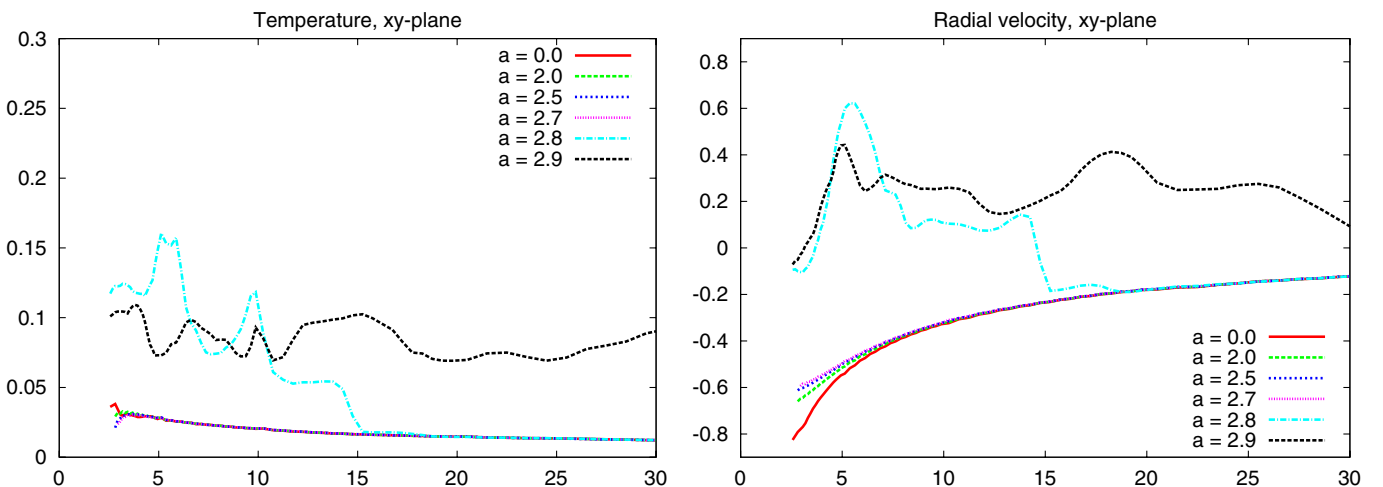

FIG. 9 (color online). Temperature and radial velocity (as seen by a local observer) as a function of the radial coordinate on the equatorial plane (xy-plane) of the accreting gas in Kerr space-time at $t = 500M$, for different values of a_*, in the case $\Gamma = 4/3$.

high spin parameters seem to be a quite robust prediction of the accretion process onto superspinars, regardless of the details of their surface. Indeed the assumption of a perfectly absorbing surface is perhaps the most conservative possibility; that is, the case in which it is more difficult to produce equatorial outflows.

Lastly, we have briefly investigated the behavior of the accretion process for a gas with a different equation of state. So far, in our study we have always assumed that the gas consists nonrelativistic particles; that is, $\Gamma = 5/3$. On the other hand, around an ordinary black hole, one should expect nonrelativistic ions and relativistic electrons. This fact could be easily implemented in our code by taking $\Gamma = 13/9$. Since here we want only to understand how our results are affected by the gas equation of state, we consider the more radical case of a gas whose pressure is dominated by relativistic particles, i.e., $\Gamma = 4/3$. The accretion process turns out to be qualitatively the same. Quantitatively, there are some differences, but that should not be a surprise, because even the standard Bondi accretion onto a Schwarzschild black hole depends on the matter equation of state. The results of our simulations for $\Gamma = 4/3$ are summarized in Fig. 9, where we show the temperature and radial velocity profile on the equatorial plane for a few different values of the spin parameter a_*. Figure 9 should be compared with Fig. 7. For $r_{\mathrm{in}} = 2.5M$, the accretion process is essentially the same for any value $|a_*| \lesssim 2.7$. For $a_* = 2.8$, there are equatorial outflows, but the gas cannot go far from the massive objects. For $a_* = 2.9$, the outflows are apparently less energetic than the ones when $\Gamma = 5/3$.

V. CONCLUSIONS

A Kerr black hole must satisfy the relation $|a_*| \leq 1$, where $a_* = J^2/M$ is the dimensionless spin parameter. So, the possible discovery of a massive and compact object with $|a_*| > 1$ would imply that the final product of the gravitational collapse is not a Kerr black hole, or at least that the Kerr solution is not the unique option. To test the bound $|a_*| \leq 1$ in astrophysical black hole candidates with electromagnetic radiation, we have to study the accretion process onto compact object either with $|a_*| \leq 1$ (black holes) and with $|a_*| > 1$ (superspinars).

In this paper, we have presented the results of our 3-dimensional general relativistic hydrodynamic simulations of adiabatic and spherically symmetric accretion in Kerr space-time. Kerr superspinars have been modeled as a compact object with radius $r \approx 2.5M$ and a surface made of exotic stuff capable of absorbing the matter hitting it: from the one hand, this choice is motivated to prevent the instability of the massive object and, from the other hand, it is inspired by a couple of scenarios proposed in the literature.

Our simulations in 3 dimensions suggest three main regimes of accretion: black hole-like state, intermediate state, and super–spinarlike state. The key elements determining the kind of accretion are the spin parameter a_* and the radius of the massive object—here the radius of the inner boundary r_{in}. However, for a smaller/larger radius, we can rescale (decrease/increase) the spin parameter and obtain a similar accretion process. For black holes and superspinars with small $|a_*|$, we find the usual picture of accretion onto black holes, with the thermodynamical variables quite independent of the actual value of a_* (black holelike state). For superspinars with moderate value of $|a_*|$, the flow around the massive object becomes subsonic and the accretion process is more difficult, making the density and the temperature of the gas increase (intermediate state). For high values of $|a_*|$, the accretion process is quite different: the superspinar accrete from the poles, while the equatorial plane is dominated by powerful outflows (super–spinarlike state).

These results confirm the findings in our previous works in 2.5 dimensions [20]. Now we can also see the details of the structure of the outflows on the equatorial plane. Although our simulations do not run for enough time to reach a quasi-steady-state equilibrium configuration in the case of high spin parameter, we argue that the accretion process onto such superspinars is characterized by the random ejections of gas in essentially all the directions, without the formation of stable structures.

[1] S. W. Hawking and G. F. R. Ellis, *The Large Scale Structure of Space-time* (Cambridge University Press, Cambridge, England, 1973).

[2] R. Penrose, Riv. Nuovo Cimento Soc. Ital. Fis. **1,** 252 (1969); Gen. Relativ. Gravit. **34,** 1141 (2002).

[3] B. Carter, Phys. Rev. Lett. **26,** 331 (1971).

[4] D. C. Robinson, Phys. Rev. Lett. **34,** 905 (1975).

[5] T. Harada and K. i. Nakao, Phys. Rev. D **70,** 041501

(2004).

[6] T. Harada, Pramana **63**, 741 (2004).

[7] D. Christodoulou, Commun. Math. Phys. **93**, 171 (1984).

[8] A. Ori and T. Piran, Phys. Rev. D **42**, 1068 (1990).

[9] P. S. Joshi and I. H. Dwivedi, Phys. Rev. D **47**, 5357 (1993).

[10] D. Christodoulou, Ann. Math. **140**, 607 (1994).

[11] I. H. Dwivedi and P. S. Joshi, Commun. Math. Phys. **166**, 117 (1994).

[12] S. S. Deshingkar, I. H. Dwivedi, and P. S. Joshi, Phys. Rev. D **59**, 044018 (1999).

[13] E. G. Gimon and P. Horava, Phys. Lett. B **672**, 299 (2009).

[14] T. Jacobson and T. P. Sotiriou, Phys. Rev. Lett. **103**, 141101 (2009); **103**, 209903(E) (2009).

[15] C. Bambi and K. Freese, Phys. Rev. D **79**, 043002 (2009).

[16] C. Bambi, K. Freese, and R. Takahashi, in *Windows on the Universe*, edited by L. Celnikier *et al.* (The Gioi Publishers, Ha Noi, Vietnam, 2010), pp. 575–578.

[17] R. Takahashi and T. Harada, Classical Quantum Gravity **27**, 075003 (2010).

[18] C. Bambi, K. Freese, T. Harada, R. Takahashi, and N. Yoshida, Phys. Rev. D **80**, 104023 (2009).

[19] C. Bambi, in *Proceedings of the Nineteenth Workshop on General Relativity and Gravitation*, edited by M. Saijo *et al.* (2010), pp. 109–112, www-tap.scphys.kyoto-u.ac.jp/jgrg/proc/JGRG19.pdf.

[20] C. Bambi, T. Harada, R. Takahashi, and N. Yoshida, Phys. Rev. D **81**, 104004 (2010).

[21] B. Carter, Phys. Rev. **174**, 1559 (1968).

[22] E. K. Boyda, S. Ganguli, P. Horava, and U. Varadarajan, Phys. Rev. D **67**, 106003 (2003).

[23] D. Israel, J. High Energy Phys. 01 (2004) 042.

[24] N. Drukker, Phys. Rev. D **70**, 084031 (2004).

[25] E. G. Gimon and P. Horava, arXiv:hep-th/0405019.

[26] P. Pani, E. Barausse, E. Berti, and V. Cardoso, Phys. Rev. D **82**, 044009 (2010).

[27] S. D. Mathur, Fortschr. Phys. **53**, 793 (2005).

[28] J. F. Hawley, L. L. Smarr, and J. R. Wilson, Astrophys. J. **277**, 296 (1984).

[29] J. F. Hawley, L. L. Smarr, and J. R. Wilson, Astrophys. J. Suppl. Ser. **55**, 211 (1984).

[30] R. F. Stark and T. Piran, Comput. Phys. Rep. **5**, 221 (1987).

[31] S. K. Chakrabarti, Phys. Rep. **266**, 229 (1996).

[32] F. C. Michel, Astrophys. Space Sci. **15**, 153 (1972).

[33] S. L. Shapiro and S. A. Teukolsky, *Black Holes, White Dwarfs, and Neutron Stars: The Physics of Compact Objects* (Wiley, New York, New York, 1983).